

Determination of the Antimony Valence State in $\text{Eu}_{10}\text{Mn}_6\text{Sb}_{13}$ Dennis E. Brown,[†] Charles E. Johnson,[†] Fernande Grandjean,[‡] Raphaël P. Hermann,[‡] Susan M. Kauzlarich,^{*§} Aaron P. Holm,[§] and Gary J. Long^{*||}

Department of Physics, Northern Illinois University, De Kalb, Illinois 60115, Department of Physics, B5, University of Liège, B-4000 Sart-Tilman, Belgium, Department of Chemistry, University of California, One Shields Avenue, Davis, California 95616, and Department of Chemistry, University of Missouri–Rolla, Rolla, Missouri 65409-0010

Received October 9, 2003

The antimony-121 Mössbauer spectra of $\text{Eu}_{10}\text{Mn}_6\text{Sb}_{13}$ have been measured between 2 and 295 K. Although the Zintl formalism indicates that the nine crystallographically distinct antimony sites in $\text{Eu}_{10}\text{Mn}_6\text{Sb}_{13}$ should have formal valence states of -2 , -1 , 0 , and $+1$, the Mössbauer spectral isomer shifts reveal that the valence states of the different sites are all quite similar and correspond to an average electronic configuration for antimony of $5s^{1.75}p^{4.0}$. This configuration corresponds to an excess of negative charge on the antimony of 0.7 or an average valence of -0.7 , a valence which is rather consistent with the average antimony valence of -0.61 obtained from the Zintl formalism for the nine antimony sites in $\text{Eu}_{10}\text{Mn}_6\text{Sb}_{13}$. The spectra obtained between 90 and 295 K are more consistent with the absence rather than the presence of any transferred magnetic hyperfine field at the antimony. In contrast, the spectra obtained at 2 and 5 K reveal the presence of an average transferred magnetic hyperfine field of ca. 8 T, a field that arises from the ferromagnetic ordering of the near-neighbor manganese(II) ions.

Introduction

Understanding the properties of the various new transition-metal-containing Zintl phase intermetallic compounds, which often have unusual and sometimes unique combinations of complex magnetic, electrical, structural, and thermal properties,¹ illustrates the importance of correlating their structural complexity with their electronic properties. One of the historically most important and simple concepts used for this correlation is that of the oxidation state of an element in a compound.

The Zintl formalism represents a generalization of the Lewis octet rule for application to either semiconducting or insulating compounds and, as such, requires charge balance between nominally closed-shell structural units, units which in themselves can be covalently or ionically bonded complexes or simple ions. This formalism has been quite useful in describing the structural, electric, and magnetic properties

of various so-called Zintl phase compounds,^{1–3} but, unfortunately, it fails in some cases. For instance, in $\text{Yb}_{14}\text{MnSb}_{11}$ the electron-counting Zintl formalism leads⁴ to a valence of $+3$ for the manganese, whereas X-ray magnetic circular dichroism at the manganese $L_{2,3}$ -edge indicates a valence of $+2$. These two different electronic configurations have been reconciled through band structure calculations⁵ on the related $\text{Ca}_{14}\text{MnBi}_{11}$ and $\text{Ba}_{14}\text{MnBi}_{11}$ Zintl compounds. In this band structure approach, the concept of formal valence is much less important than in the Zintl formalism and orbital hybridization and electron density become the important parameters for describing the electronic structure of a compound.

In a recent paper⁶ we have reported the structural, electronic, and magnetic properties of a new ternary rare-earth

* To whom correspondence should be addressed. E-mail: glong@umr.edu (G.J.L.).

[†] Northern Illinois University.

[‡] University of Liège.

[§] University of California.

^{||} University of Missouri–Rolla.

(1) Kauzlarich, S. M.; Payne, A. C.; Webb, D. J. In *Magnetism: Molecules to Materials III*; Miller, J. S., Drillon, M., Eds.; Wiley-VCH: Weinheim, Germany, 2002; pp 37–62.

(2) Kim, S.-J.; Hu, S.; Uher, C.; Kanatzidis, M. G. *Chem. Mater.* **1999**, *11*, 3154–3159.

(3) Chung, D.-Y.; Hogan, T.; Brazis, P.; Rocci-Lane, M.; Kannewurf, C.; Bastea, M.; Uher, C.; Kanatzidis, M. G. *Science* **2000**, *287*, 1024–1027.

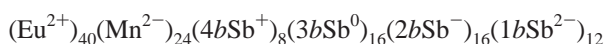
(4) Holm, A. P.; Kauzlarich, S. M.; Morton, S. A.; Waddill, G. D.; Pickett, W. E.; Tobin, J. G. *J. Am. Chem. Soc.* **2002**, *124*, 9894–9898.

(5) Sánchez-Portal, D.; Martin, R. M.; Kauzlarich, S. M.; Pickett, W. E. *Phys. Rev. B* **2002**, *65*, 144414–15.

(6) Holm, A. P.; Park, S.-M.; Condrón, C. L.; Olmstead, M. M.; Kim, H.; Klavins, P.; Grandjean, F.; Hermann, R. P.; Long, G. J.; Kanatzidis, M. G.; Kauzlarich, S. M.; Kim, S.-J. *Inorg. Chem.* **2003**, *43*, 4660–4667.

transition-metal Zintl compound, $\text{Eu}_{10}\text{Mn}_6\text{Sb}_{13}$, a compound which contains *seven* crystallographically distinct europium sites, *four* crystallographically distinct manganese sites, and *nine* crystallographically distinct antimony sites. Thus, $\text{Eu}_{10}\text{Mn}_6\text{Sb}_{13}$ surely has a complex structure in which the same metal could well have different oxidation states or valence states in different crystallographic sites.

According to the Zintl formalism, in $\text{Eu}_{10}\text{Mn}_6\text{Sb}_{13}$ the formal charge of the 12 singly bonded *4i* Sb(3), *4i* Sb(6), and *4i* Sb(8) sites can be assigned⁶ as Sb(−II), the 16 doubly bonded *4i* Sb(1), *4i* Sb(7), and *8j* Sb(9) sites can be assigned as Sb(−I), the 16 triply bonded *8j* Sb(4) and *8j* Sb(5) sites can be assigned as Sb(0), and the 8 quadruply bonded *8j* Sb(2) sites can be assigned as Sb(I), where the crystallographic sites are labeled the same as in ref 6. This assignment yields an average antimony valence of −0.61. Hence, the antimony atoms are subdivided in four groups with different formal oxidation states, −2, −1, 0, and +1, in the ratio of 12:16:16:8 or 3:4:4:2 within the Zintl formalism. The use of these formal charges reflects the Zintl viewpoint that the bonding between the manganese and antimony in the anionic framework is covalent. Because the chemical behavior of Mn(II) is very similar to that of Zn(II) in other Zintl phases, for electron-counting purposes, the manganese in $\text{Eu}_{10}\text{Mn}_6\text{Sb}_{13}$ may be substituted with zinc; i.e., the manganese(II) $3d^5$ electrons may be ignored. Thus, $\text{Eu}_{10}\text{Mn}_6\text{Sb}_{13}$ can be considered as a valence precise compound and can be described as



where *b* represents the number of antimony bonds. The use of Mn(−II) in this formulation may seem unusual but is required to achieve charge balance with the positive charges of europium and the antimony charges, which have been assigned according to the Zintl formalism.

In our earlier work⁶ we have used the europium-151 Mössbauer spectra to show that all seven of the europium sites have very similar valence states of essentially +2 and that six of the seven europium sites undergo magnetic ordering at higher temperatures than the seventh site. Because the oxidation state of manganese is likely to be +2, as is implied both by the magnetic susceptibility of $\text{Eu}_{10}\text{Mn}_6\text{Sb}_{13}$, assuming that the manganese ions are antiferromagnetically coupled⁶ and by the magnetic properties observed^{4,5} in other Zintl phases, it is important to determine the formal valence state of the antimony in $\text{Eu}_{10}\text{Mn}_6\text{Sb}_{13}$ and hence to evaluate the adequacy of the Zintl formalism in describing its metallic conductivity below 40 K and semiconductivity above 60 K.

Antimony-121 Mössbauer spectroscopy is an ideal technique^{7,8} to selectively probe the electronic configuration of the antimony in $\text{Eu}_{10}\text{Mn}_6\text{Sb}_{13}$ and the magnetic interactions of antimony with its europium and manganese neighbors through the isomer shift and transferred magnetic hyperfine

Table 1. Antimony-121 Mössbauer Spectral Parameters

compd	T, K	δ , ^a mm/s	Γ , mm/s	H, T	area, (% ϵ)(mm/s)
$\text{Eu}_{10}\text{Mn}_6\text{Sb}_{13}$	295	−8.13(5)	2.23 ^b	0 ^b	5.5(2)
	220	−8.16(5)	2.23 ^b	0 ^b	12.7(3)
	165	−8.16(5)	2.23 ^b	0 ^b	23.5(2)
	125	−8.20(5)	2.23 ^b	0 ^b	34.4(2)
	90	−8.15(5)	2.23 ^b	0 ^{b,c}	49.3(4)
	5	−8.14(5)	2.23 ^b	7.95(9)	83.2(5)
InSb	2	−8.15(5)	2.23 ^b	8.3(1)	82(2)
	295	−8.73(4)	2.23(12)	0 ^b	3.5(1)
InSb	90	−8.60(1)	2.73(3)	0 ^b	60.4(5)
	5	−8.54(1)	3.32(3)	0 ^b	113.4(7)

^a The isomer shift is given relative to the CaSnO_3 source at room temperature. ^b Parameter constrained to the value given. ^c Alternative fits (see text) yield a maximum field of 3.3(1) T.

field, respectively. Herein, we report the antimony-121 Mössbauer spectra obtained for $\text{Eu}_{10}\text{Mn}_6\text{Sb}_{13}$.

Experimental Methods

The sample of $\text{Eu}_{10}\text{Mn}_6\text{Sb}_{13}$ used in this work is the same as that used in our previous study.⁶

The Mössbauer spectra were obtained with a conventional constant-acceleration spectrometer which utilized a room-temperature ca. 0.2 mCi tin-121* in CaSnO_3 source and was calibrated at room temperature with α -iron foil and InSb. The absorber was mounted in the vacuum space of a Janis liquid-helium cryostat, and its temperature was controlled by a commercial sensor and heater.

The $\text{Eu}_{10}\text{Mn}_6\text{Sb}_{13}$ Mössbauer spectral absorber thickness was 32 mg/cm² of sample or 8 mg/cm² of antimony. An absorber containing 16 mg/cm² of $\text{Eu}_{10}\text{Mn}_6\text{Sb}_{13}$ gave hyperfine parameters at 90 K that are essentially identical with those given in Table 1. The InSb absorber thickness was 31 mg/cm² of sample or 16 mg/cm² of antimony.

The hyperfine parameters for InSb are given in Table 1 for comparison. The InSb line width of 2.23(12) mm/s observed at 295 K was used for all subsequent spectral fits. All isomer shifts are given relative to the CaSnO_3 source, values which are identical with those given relative to BaSnO_3 .

Results and Discussion

The antimony-121 Mössbauer spectra of $\text{Eu}_{10}\text{Mn}_6\text{Sb}_{13}$ obtained between 2 and 295 K are shown in Figure 1, and the associated spectral hyperfine parameters are given in Table 1. From the results shown in Figure 1 it is immediately apparent that antimony-121 Mössbauer spectroscopy is unable to distinguish between the nine crystallographically distinct antimony sites in $\text{Eu}_{10}\text{Mn}_6\text{Sb}_{13}$, in part because of its intrinsic and experimentally limited resolution; the minimum possible antimony-121 spectral line width, the Heisenberg line width, is 2.10(12) mm/s.

A preliminary fit of the Mössbauer spectra obtained between 90 and 295 K with a single Lorentzian line indicated the presence of a small asymmetry in the spectra. Clearly, the analysis of such spectra is complex in view of the nine different antimony sites present in $\text{Eu}_{10}\text{Mn}_6\text{Sb}_{13}$, sites that may all have different isomer shifts and quadrupole interactions. As a consequence, we have elected to fit the $\text{Eu}_{10}\text{Mn}_6\text{Sb}_{13}$ 90–295 K spectra with nine Lorentzian singlets with the proper degeneracy and a line width of 2.23 mm/s but to report only the average $\text{Eu}_{10}\text{Mn}_6\text{Sb}_{13}$ isomer shift. This

(7) Ruby, S. L.; Shenoy, G. K. In *Mössbauer Isomer Shifts*; Wagner, F. E., Shenoy, G. K., Eds.; North-Holland: Amsterdam, 1978; pp 617–659.

(8) Grandjean, F.; Long, G. J.; Longworth, G.; Laundry, B. J. *Inorg. Chem.* **1984**, *23*, 1886–1895.

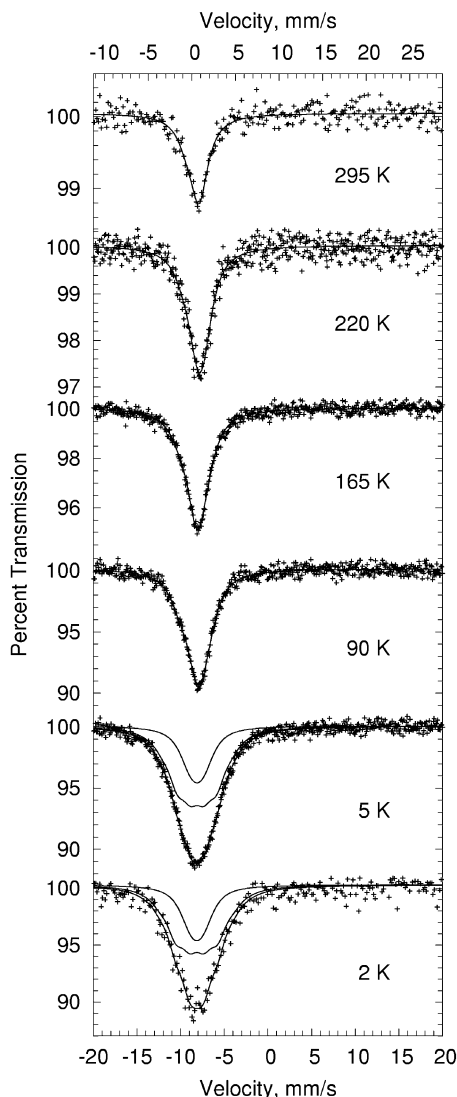


Figure 1. Antimony-121 Mössbauer spectra of $\text{Eu}_{10}\text{Mn}_6\text{Sb}_{13}$ obtained at the indicated temperatures. The lower velocity scale corresponds to the velocity relative to the CaSnO_3 source, and the upper scale corresponds to the velocity relative to InSb .

approach yields an isomer shift that is independent of temperature as is shown in Table 1.

The average isomer shift for the nine antimony sites in $\text{Eu}_{10}\text{Mn}_6\text{Sb}_{13}$ is -8.15 ± 0.05 mm/s relative to the CaSnO_3 source, a value which is somewhat higher than that obtained for InSb at 295 K. The significance of the isomer shift in revealing the electronic properties of $\text{Eu}_{10}\text{Mn}_6\text{Sb}_{13}$, is discussed below.

At 90 K and perhaps at temperatures up to 220 K the four manganese(II) sublattices in $\text{Eu}_{10}\text{Mn}_6\text{Sb}_{13}$ are expected⁶ to be antiferromagnetically coupled and any resulting transferred hyperfine field at the antimony sites should be small. It should be noted that, except for Sb(7) and Sb(8), all the antimony ions are directly bonded to the manganese(II) ions. Because it is possible that the antimony is experiencing a small transferred hyperfine field from the antiferromagnetically ordered manganese ions in $\text{Eu}_{10}\text{Mn}_6\text{Sb}_{13}$, we have undertaken an alternative fit of its 90 K spectrum, a fit which uses one hyperfine field rather than the nine singlets. The

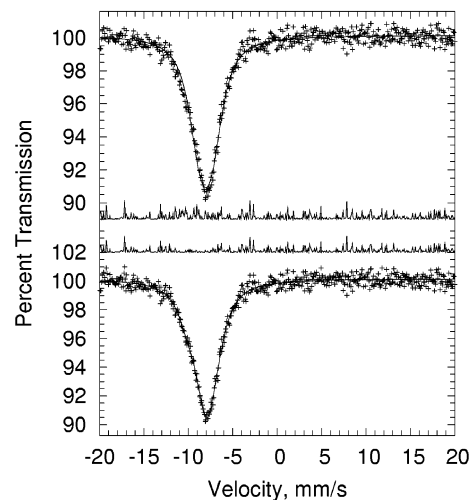


Figure 2. Antimony-121 Mössbauer spectra of $\text{Eu}_{10}\text{Mn}_6\text{Sb}_{13}$ obtained at 90 K and fit with one magnetic component with a hyperfine field of 3.3(1) T, upper plot, and with nine singlets, lower plot. The fit residuals for the respective fits are shown in the center. The velocity scale corresponds to the velocity relative to the CaSnO_3 .

resulting fit, which yields a field of 3.3(1) T, is shown in the upper portion of Figure 2. Although this approach does not rule out the presence of a small transferred field at 90 K on some of the sites, we believe that the spectrum is more realistically fit with no transferred hyperfine field, as is shown in the lower portion of Figure 2.

The fits of the $\text{Eu}_{10}\text{Mn}_6\text{Sb}_{13}$ Mössbauer spectra obtained at 2 and 5 K and shown in Figure 1 have been obtained using two magnetic components indicating that the transferred hyperfine field may be somewhat different at the differing antimony sites. It is difficult to determine whether all nine of the antimony sites in $\text{Eu}_{10}\text{Mn}_6\text{Sb}_{13}$ experience the same or differing transferred hyperfine fields, although structural considerations⁶ would indicate that differences are possible. In an attempt to determine whether one or more transferred fields are present at 5 K, we have attempted an alternative fit with one field; see the upper portion of Figure 3. As is shown in this figure, the fit with one transferred field is marginal and we believe that the spectrum is best fit with more than one transferred field. But, once again, because of the large number of antimony sites, only the average transferred hyperfine field will have any physical significance.

At 2 and 5 K, temperatures which are below the ferromagnetic ordering temperature⁶ of all seven europium sublattices, the transferred field on the antimony atoms is, as expected, substantial at ca. 7.95(9) and 8.3(1) T, respectively. Because no thickness correction has been applied to these spectra, the reported fields should be considered as the upper limit of the transferred field. These transferred fields are at most half the supertransferred hyperfine fields observed⁸ in spinel antimonates, in which the transfer of the electron spin density takes place through the Fe(III)—O—Sb(V) bonding. There are rather few cases for which the transferred field at antimony in a magnetic intermetallic compound or alloy has been measured. For the diamagnetic antimony impurity in α -iron, a transferred field of 24.5 T has been observed.⁹ In the ferromagnetic Pd_2MnSb ,

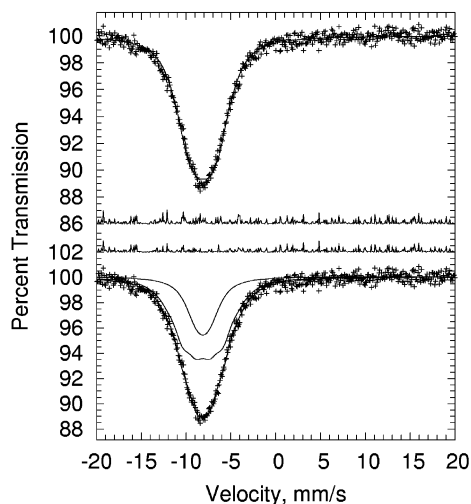


Figure 3. Antimony-121 Mössbauer spectra of $\text{Eu}_{10}\text{Mn}_6\text{Sb}_{13}$ obtained at 5 K and fit with one magnetic component with a hyperfine field of 7.66(7) T, upper plot, and with two magnetic components with a weighted average hyperfine field of 7.95(9) T, lower plot. The velocity scale corresponds to the velocity relative to the CaSnO_3 .

PdMnSb , and NiMnSb compounds transferred fields of 57.9, 30.2, and 29.1 T, respectively, have been observed¹⁰ at 100 K. Finally, the transferred hyperfine field at antimony in the $\text{Mn}_{1-x}\text{Cr}_x\text{Sb}$ series has been measured¹¹ as a function of x . In the ferromagnetic phase, for x less than 0.25, fields between 38 and 19 T have been observed, whereas in the antiferromagnetic phase, for $x = 0.9$, a much smaller field of 5.2 T has been observed.

In all the above compounds, the transfer of the electron spin density takes place between the manganese 3d orbitals and the antimony 5s and 5p orbitals. In the ferromagnetic compounds, this transfer is quite efficient and may be enhanced by a small magnetic moment on the Pd and, hence, leads to large or even giant transferred hyperfine fields of 20–60 T. In antiferromagnetic $\text{Mn}_{0.1}\text{Cr}_{0.9}\text{Sb}$ the antiferromagnetic coupling of the moments leads to a small transferred hyperfine field of 5.2 T, probably because the antimony atom has magnetic near neighbors with antiparallel moments, which contribute transferred fields of opposite sign, in a fashion similar to that observed¹² in YFe_6Sn_6 .

In $\text{Eu}_{10}\text{Mn}_6\text{Sb}_{13}$ between 90 and 220 K, the manganese magnetic moments are expected to be antiferromagnetically coupled and, at most, only a very small transferred field through the overlap of the manganese 3d with the antimony 5s orbitals should be observed. At 2 and 5 K the europium magnetic moments are ferromagnetically ordered and a larger transferred field of ca. 8 T is observed. In this case, the transfer of the electron spin density takes place through overlap of the europium 4f and the antimony 5s orbitals. Because the europium 4f orbitals have a rather small spatial extension, this transfer is not very efficient and the measured transferred hyperfine field is much smaller than in the

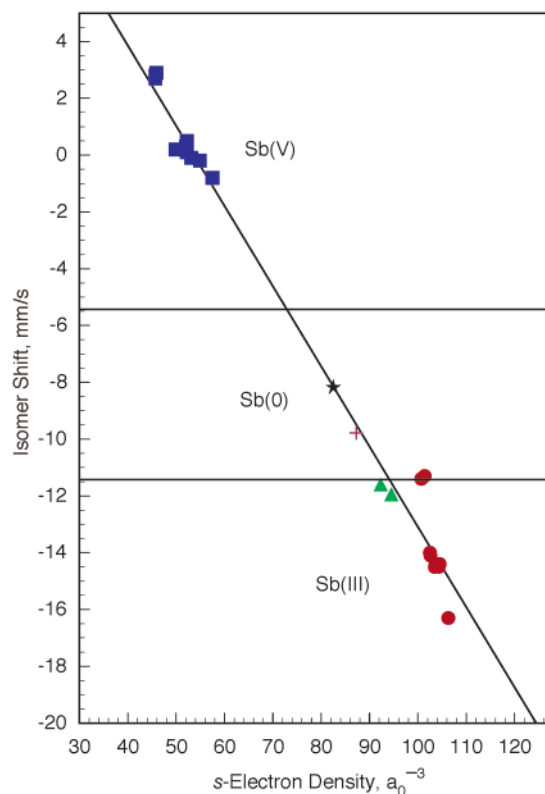


Figure 4. Correlation between the experimental values of the antimony-121 Mössbauer-effect isomer shift, relative to CaSnO_3 , and the calculated values of the electron density at the nucleus for the Sb(V), squares, Sb(0), triangles, and Sb(III), circles, compounds. The data are taken from ref 13. The star corresponds to $\text{Eu}_{10}\text{Mn}_6\text{Sb}_{13}$, and the plus, to the value obtained from ref 14 for CoSb_3 .

manganese containing ferromagnetic compounds mentioned above. Because $\text{Eu}_{10}\text{Mn}_6\text{Sb}_{13}$ exhibits some metallic conductivity below 40 K, it is quite possible that the transfer of the spin density can also be assisted by a RKKY type interaction, which includes the conduction electrons.

The observed isomer shift of -8.15 ± 0.05 mm/s relative to CaSnO_3 occurs in the range of isomer shifts observed for the Sb^0 valence state in antimony semiconducting compounds, such as InSb , as is illustrated in Figure 4. In this figure, the observed¹³ isomer shift in various Sb(V), Sb(0), and Sb(III) compounds has been plotted as a function of the calculated electron density, $\rho(0)$, at the antimony nucleus. The observed isomer shift for $\text{Eu}_{10}\text{Mn}_6\text{Sb}_{13}$ is shown by the star in Figure 4. The linear correlation shown in Figure 4 yields for $\text{Eu}_{10}\text{Mn}_6\text{Sb}_{13}$ an average $\rho(0)$ value of $82.5a_0^{-3}$, where a_0 is the Bohr radius, or 587 \AA^{-3} . This density is at the lower limit of the densities calculated¹³ for Sb^0 compounds. To support our present analysis, the observed¹⁴ isomer shift for CoSb_3 , for which band structure calculations¹⁵ are available, is also plotted as a plus in Figure 4. The linear correlation yields a valence electron density, $\rho(0)$, of $87.3a_0^{-3}$ or 621 \AA^{-3} for CoSb_3 .

(9) Ruby, S. L.; Johnson, C. E. *Phys. Lett.* **1967**, *26A*, 60–61.
 (10) Swartzendruber, L. J.; Evans, B. J. *Phys. Lett.* **1972**, *38A*, 511–512.
 (11) Pasternak, M.; Vernes, P. *Solid State Commun.* **1974**, *15*, 1189–1191.
 (12) Cadogan, J. M.; Suharyana; Ryan, D. H.; Moze, O. *J. Appl. Phys.* **2000**, *87*, 6045–6047.

(13) Lippens, P. E. *Solid State Commun.* **2000**, *113*, 399–403.
 (14) Aldon, F.; Garcia, A.; Olivier-Fourcade, J.; Jumas, J.-C.; Fernández-Madrugal, F. J.; Lavela, P.; Vicente, C. P.; Tidaó, J. L. *J. Power Sources* **2003**, *119–121*, 585–590.
 (15) Lefebvre-Devos, I.; Lasalle, M.; Wallart, X.; Olivier-Fourcade, J.; Monconduit, L.; Jumas, J.-C. *Phys. Rev. B* **2001**, *63*, 125110–7.

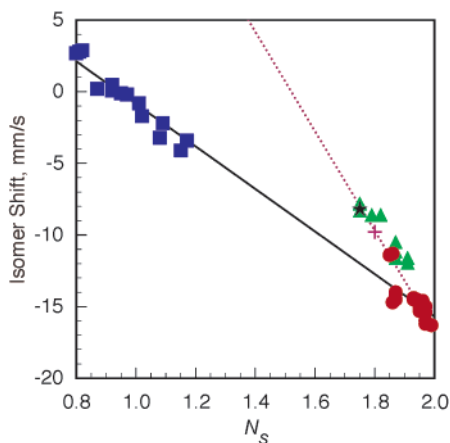


Figure 5. Correlation between the experimental values of the antimony-121 Mössbauer-effect isomer shift, relative to CaSnO_3 , and the calculated number of antimony 5s electrons, N_s , for the Sb(V), squares, Sb(0), triangles, and Sb(III), circles, compounds. The solid line represents a fit to the Sb(V) and Sb(III) data, whereas the dotted line represents a fit to the Sb(0) and Sb(III) data points. The data are from ref 13. The star corresponds to $\text{Eu}_{10}\text{Mn}_6\text{Sb}_{13}$, and the plus, to the value obtained from ref 14 for CoSb_3 .

Lippens¹³ has also shown that there are linear correlations between the antimony-121 isomer shift and the calculated number of antimony 5s electrons, as is shown in Figure 5 for the same compounds used in Figure 4. First, there is a linear correlation between the Sb(V) and Sb(III) compounds, a correlation which illustrates the predominate influence of the number of 5s electrons on the antimony-121 Mössbauer-effect isomer shift. Second, there is a different linear correlation between the Sb⁰ and Sb(III) compounds, a correlation which illustrates the secondary effect of screening of the antimony 5p electrons on the isomer shift. This correlation yields 1.8 and 1.7 electrons for the number of antimony 5s electrons, N_s , in CoSb_3 and $\text{Eu}_{10}\text{Mn}_6\text{Sb}_{13}$, respectively. The value of 1.8 electrons for CoSb_3 agrees very well with the calculated¹⁵ value of 1.77. This agreement provides confidence in the application of the correlations in Figures 4 and 5 to $\text{Eu}_{10}\text{Mn}_6\text{Sb}_{13}$.

Ruby and Shenoy⁷ have given the expression

$$\rho(0) = 0.11 + 68.65N_s - 3.39N_p - 5.57N_s^2 - 1.00N_sN_p \quad (1)$$

for $\rho(0)$ as a function of the numbers of 5s and 5p electrons in antimony. From eq 1 and the values of $\rho(0)$ and N_s obtained from the linear fits shown in Figures 4 and 5, we find that N_p is 4.0 and, thus, that the average electronic configuration of antimony in $\text{Eu}_{10}\text{Mn}_6\text{Sb}_{13}$ is $5s^{1.75}p^{4.0}$. This is an excess of negative charge on the antimony of 0.7 or a formal average valence of -0.7 , a valence that is rather consistent with the formal average valence of -0.61 obtained from the Zintl formalism.

Antimony-121 Mössbauer spectroscopy fails to distinguish the different antimony valence states in $\text{Eu}_{10}\text{Mn}_6\text{Sb}_{13}$ predicted from the Zintl formalism partly because of its inherently low resolution. However, the expected differences in the isomer shifts between the four predicted valence states, Sb^+ , Sb^0 , Sb^- , and Sb^{2-} , are small. Indeed, if the 5s state is reasonably assumed fully occupied, the expected correspond-

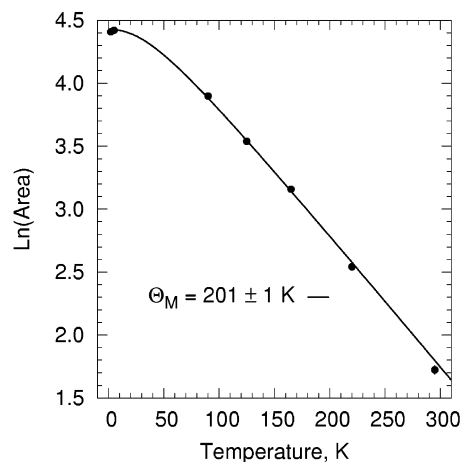


Figure 6. Temperature dependence of the antimony-121 Mössbauer spectral absorption area observed for $\text{Eu}_{10}\text{Mn}_6\text{Sb}_{13}$ and fit with a Debye model for the recoil-free fraction.

ing electron configurations are $5s^25p^2$, $5s^25p^3$, $5s^25p^4$, and $5s^25p^5$, and they differ only by the number, N_p , of 5p electrons. Equation 1 and Figure 4 show that the influence of N_p on the isomer shift is smaller than that of N_s ; the influence of N_p is well illustrated in Figure 5, which indicates that the Sb(0) and Sb(III) compounds have similar N_s and different N_p values. Indeed, N_p varies¹³ only between 1.22 and 2.11 and 3.09 and 3.51 for the Sb(III) and Sb(0) compounds, respectively. From eq 1 and the linear fit in Figure 4, the expected isomer shifts for the four valence states, Sb(I), Sb(0), Sb(−I), and Sb(−II), are -14.8 , -13.2 , -11.6 , and -10.1 mm/s, respectively. At 90 K the spread in isomer shifts of ca. 4.7 mm/s is difficult to distinguish from the effect of a transferred hyperfine field from the manganese or europium with an experimental line width of 2.23 mm/s.

The temperature dependence of the Mössbauer spectral absorption area can provide information about the lattice properties of a compound.^{16–18} A plot of the logarithm of the antimony-121 spectral absorption area for $\text{Eu}_{10}\text{Mn}_6\text{Sb}_{13}$ as a function of temperature is close to linear at higher temperatures, as is shown in Figure 6. A fit with the Debye model for the recoil-free fraction¹⁶ leads to an effective Mössbauer lattice temperature, Θ_M , of 201(1) K, a value which is typical of an intermetallic compound such as $\text{Eu}_{10}\text{Mn}_6\text{Sb}_{13}$ and is only slightly higher than the value of 160(5) K obtained¹⁹ for InSb.

An analogous fit of the Mössbauer spectral absorption area observed herein for InSb leads to an effective Mössbauer lattice temperature, Θ_M , of 175(4) K. This value is somewhat higher than the 160(5) K value observed earlier because no saturation correction has been applied in our work. It should be noted that the 11–160 K isomer shift of $-8.56(5)$ mm/s reported earlier¹⁹ for InSb is in excellent agreement with the 90 and 5 K values observed herein and given in Table 1.

(16) Herber, R. H. In *Chemical Mössbauer Spectroscopy*; Herber, R. H., Ed.; Plenum Press: New York, 1984; pp 199–216.

(17) Long, G. J.; Hautot, D.; Grandjean, F.; Morelli, D. T.; Meisner, G. P. *Phys. Rev. B* **1999**, *60*, 7410–7418.

(18) Long, G. J.; Hautot, D.; Grandjean, F.; Morelli, D. T.; Meisner, G. P. *Phys. Rev. B* **2000**, *62*, 6829–6831.

(19) Hedges, S. W.; Bowen, L. H. *Mater. Sci. Forum* **1984**, *2*, 65–80.

In conclusion we find that antimony-121 Mössbauer spectroscopy is an excellent method by which to determine the average valence state of antimony in a compound which may or may not have differing antimony valence or oxidation states. However, it should be noted that because of the inherent line width of the antimony-121 transition, it is not easy to distinguish different antimony valence states in the same compound. It is also effective in measuring the transferred hyperfine field at the antimony sites in a ferromagnetically ordered compound. In $\text{Eu}_{10}\text{Mn}_6\text{Sb}_{13}$ the average electronic configuration of antimony is $5s^{1.7}5p^{4.0}$, a configuration which corresponds to an average antimony valence

of -0.7 , a valence which is consistent with the formal average valence of -0.61 obtained from the Zintl formalism.

Acknowledgment. The authors thank Sung-Jin Kim for helpful discussions during the course of this work. G.J.L. thanks the Francqui Foundation of Belgium for his appointment as a “Chaire Francqui Interuniversitaire au titre étranger” during the 2002–2003 academic year. This work was supported in part by the State of Illinois through a HECA grant.

IC035172M